Hydrothermal synthesis of a new ethylenediammonium intercalated vanadyl phosphate, $(H_3NCH_2CH_2NH_3)_{0 \cdot 5}[V^{4+}_{0 \cdot 32}V^{5+}_{0 \cdot 68}O_2PO_4\{P(OH)_2\}_{0 \cdot 44}]$
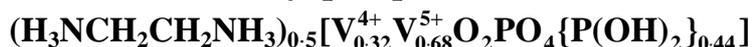
P AYYAPPAN[a], MINAKSHI ASNANI[a], A RAMANAN[a]* and Y PIFFARD[b]
[a]Department of Chemistry, Indian Institute of Technology, New Delhi 110 016, India
[b]Institut des Matériaux de Nantes, Laboratoire de Chimie des Solides, CNRS, University of Nantes, France
e-mail: aramanan@chemistry.iitd.ernet.in

Abstract. In this paper we report the hydrothermal synthesis and characterisation of a new ethylenediammonium intercalated vanadyl phosphate, $(H_3NCH_2CH_2NH_3)_{0 \cdot 5}[V^{4+}_{0 \cdot 32}V^{5+}_{0 \cdot 68}O_2PO_4\{P(OH)_2\}_{0 \cdot 44}]$. The phase purity of the solid was established using powder X-ray diffraction, single crystal X-ray diffraction, TGA, DTA, FTIR, UV-Vis and magnetic susceptibility measurements. Crystal data: orthorhombic, *Pnma*, $a = 9 \cdot 0289$, $b = 8 \cdot 8962$ and $c = 15 \cdot 9813$ Å, $V = 1283 \cdot 7$Å^3, $Z = 8$. The structure contains layers made of VO$_5$ square pyramids and PO$_4$ tetrahedra; adjacent layers are connected through disordered tetrahedral PO$_2$(OH)$_2$ units. Ethylenediammonium cations occupy cavities in between the layers.

Keywords. Vanadyl phosphate; hydrothermal synthesis; intercalation; single crystal structure.

1. Introduction

Vanadyl phosphates are important catalytic materials.[1] Hydrothermal synthesis is a popular low temperature chemical route for preparing novel vanadyl phosphates.[2–6] Ethylenediamine (*en*) is one of the commonly employed template or structure-directing molecules during the hydrothermal synthesis of vanadyl phosphates. Several vanadyl phosphates (1D ribbons, 2D layers and 3D network) have been reported to form in the presence of '*en*'.[7–15] In all these solids *en* molecules occur in suitable cavities either as diprotonated or mono-protonated cations invariably in *trans* configuration and show weak to medium hydrogen bonding with the host lattice. We have been investigating the formation of new intercalated vanadyl phosphates in the presence of ethylenediamine, metal powder and metal complex. In this paper, we report the synthesis of $(H_3NCH_2CH_2NH_3)_{0 \cdot 5}[V^{4+}_{0 \cdot 32}V^{5+}_{0 \cdot 68}O_2PO_4\{P(OH)_2\}_{0 \cdot 44}]$, *en*VPO and its full characterisation.

_____

*For correspondence

2.   Experimental

In all our preparations, reagent grade chemicals were used without further purification. The phases were further characterised by FTIR (Nicolet 5DX), powder X-ray diffraction (Bruker AXS), TGA (Perkin-Elmer, TGA7), DTA (Perkin-Elemer, DTA7), ESR (Bruker ER 200D), EDAX (Philips Model PV9900), SEM (Cambridge Stereoscan 360) and magnetic susceptibility measurements (SQUID magnetometer).

2.1   *Synthesis of enVPO*

V_2O_5 (0·2 g) was reacted with 0·0516 g Ni powder, 2 ml H_3PO_4, 0·17 ml of *en* and 30 ml distilled water in the molar ratio $V_2O_5 : Ni : H_3PO_4 : en : H_2O = 1 : 1 : 32·4 : 2.4 : 1515$. We also attempted to prepare the samples in presence of Mg, Fe, Co, Cu, Zn, Ag, and Sn. In all the cases, the mixture was transferred to a 45 ml Teflon lined Parr acid digestion reactor, which was heated at 180°C for 10 h under autogenous pressure before cooling to room temperature at 10°C/h. The resulting green crystals were washed with distilled water, acetone and allowed to dry in air. Under optical microscopic examination, the phase appeared to be homogeneous.

2.2   *X-ray crystallographic studies*

Single-crystal diffraction studies were carried out on a Siemens SMART CCD diffractometer with an MoK*a* sealed tube at 22°C. Experimental conditions for *en*VPO are given in table 1. A crystal with dimensions of $0·30 \times 0·20 \times 0·05$ mm was used for diffraction experiments. A total of 8313 reflections were collected in the theta range

Table 1.   Crystallographic data for *en*VPO.

Chemical formula	$(H_3NCH_2CH_2NH_3)_{0·5}[VO_2(PO_4)\{P(OH)_2\}_{0·44}]$
Formula weight	332·55
Crystal system	Orthorhombic
Space group	*Pnma*
a (Å)	9·0289 (2)
b (Å)	8·8962 (3)
c (Å)	15·9813 (7)
V (Å^3)	1283·7 (4)
Temperature (K)	295
Z	8
r_{calc}(g cm^{-3})	3·4408
l (Å)	0·71073
q range ($^\circ$)	2·06–29·0
Total data	8313
Total unique data	1733
Observed data [$I > 3s(I)$]	1319
$R_1[I > 3s(I)]$	4·69
wR_2	6·69
F (000)	898
GOF	2·91

$R_1 = (\||Fo|–|Fc|\|)/(|Fo|)$; $wR_2 = [w(Fo^2–Fc^2)/(wFo^4)]^{1/2}$; $GOF = [w(Fo^2–Fc^2)^2/(n–p)]^{1/2}$ where n is the number of reflections and p is the number of parameters refined

2·06–29·0°. SADABS software was used for absorption correction and SHELXTL for space group, structure determination and refinements.[17] The structure was refined from the data collected on two samples prepared in the presence of copper and nickel. Both chemical and single crystal data confirm that the crystals belong to the same compound. Structure refinement was first carried out in the space group *Cmca*, one of the possible space groups according to the systematic extinctions. Initial structure revealed the presence of layered [VO$_2$PO$_4$] units as seen in other vanadyl phosphates. Since we were unable to rationalise the remaining electron density in terms of the organic groups, we examined several other lower symmetry space groups – *Pmnb*, *P2$_1$nb* etc. to locate the ethylenediammonium cations precisely. Based on chemical analysis and EDAX, we inferred that only ethylenediammonium cations are present in the solid in addition to vanadium, phosphorous and oxygen. There was no metal incorporation and hence the presence of metal ethylenediamine complex is ruled out. Except for the space group *Pmnb*, the structural models invariably resulted in poorer *R* values with unrealistic bond distances. A close examination of the difference fourier map revealed the presence of a phosphate unit linking the vanadyl phosphate layers. Interestingly, both the organic cations as well as the phosphate groups occurring in between the layers are disordered.

3. Results and discussion

X-ray powder patterns of all the phases prepared in the presence of ethylene diamine are quite similar exhibiting lamellar characteristics with an interlayer distance of ∼ 8 Å (figure 1). Even though different metal powders were used as reducing agents, the phases did not contain any metal other than V and P as confirmed by AAS and EDAX analysis. *en*VPO forms even in the absence of metal; metal seems to assist the growth of well-defined crystals. On the basis of chemical analysis, powder XRD and TGA, we infer that under our reaction condition, only *en*VPO is formed. FTIR of *en*VPO shows characteristic features of ethylenediammonium ion: peaks in the region 2960–2850, 1340, 3500, 1650–1590, 1220–1020 cm^{-1} correspond to C–H stretching, C–H bending, N–H stretching, N–H bending and C–N (aliphatic) stretching respectively. TGA (figure 2)
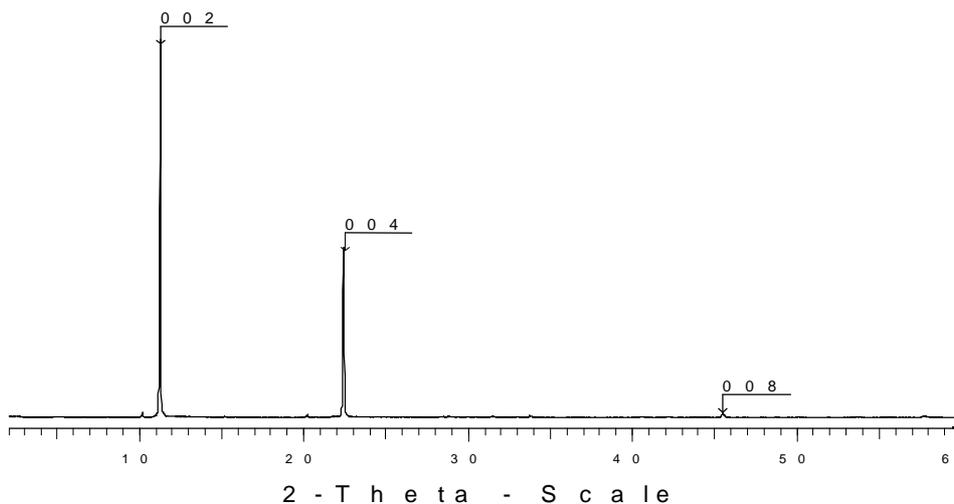
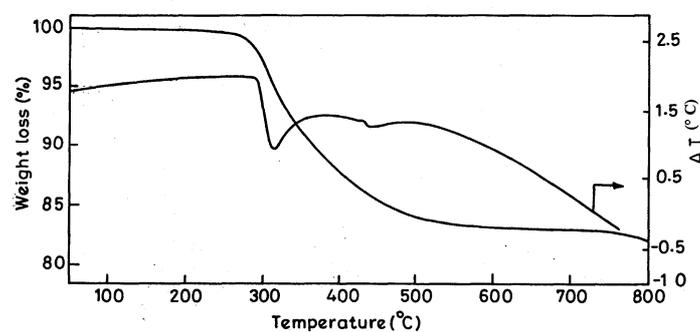**Figure 1.** Powder X-ray diffraction pattern of *en*VPO.

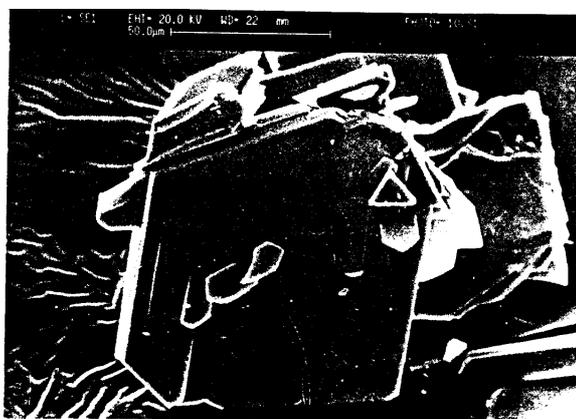**Figure 2.**   TG and DTA curves for *en*VPO.

Figure 3.   SEM photograph of *en*VPO.

shows a broad weight loss at temperatures in the range 280–500°C corresponding to the decomposition of ethylenediammonium cation while DTA shows a broad endothermic peak around 320°C. Powder XRD of *en*VPO heated around 350°C is X-ray amorphous. CHN analysis confirms the presence of C and N with the ratio 1 : 1. EDAX analysis of all the samples confirms the absence of metal other than vanadium. ESR of the samples shows a broad signal with $g \sim 1.98$ similar to other vanadyl phosphates.[16] Cerimetric titrations shows vanadium to be in mixed-valent state ($V^{4+}/V^{5+} = 0.46$). Ethylene diamine reduces vanadium(V) to the lower oxidation state V(IV) which is well-documented in the literature.[7–15] On the basis of chemical analysis and powder XRD, we confirmed that all the preparations lead to only *en*VPO. The exact composition of the phase *en*VPO was derived from single crystal structure refinement. SEM photographs (figure 3) show different habits from that of other metal-intercalated layered vanadyl phosphates.

3.1   *Crystal structure of enVPO*

Structure solution using SHELXTL gave the coordinates of V1, V2, P3 and O8. These positions were successfully refined to arrive at the structure of anionic layers which is

$[V_8P_8O_{48}]^{n-}$ (for one unit cell). All these positions are fully occupied. Bond valence calculations[18] showed that V1 is about $+4\cdot3$, and V2 is very close to $+5$. This approximates the charge of the anionic layer as around $-18\cdot8$. The value is comparable to the average oxidation state of vanadium $(+4\cdot68)$ estimated from chemical analysis. A careful analysis of the difference Fourier suggested additional phosphate groups in between the layers. Attempts to refine the position of these P atoms indicated a possible disorder. A meaningful phosphate tetrahedral geometry with acceptable bond distances was arrived only when we considered 50% disorder for the P2 (8d) position. This position cannot be fully occupied at the same time as it will lead to a P-P distance of $1\cdot53$ Å. Further refinement showed that the occupancy of the P atoms is close to $0\cdot44$. To define the oxygen tetrahedron around P2, we constrained the occupancy of O9 and O10 positions to P2. Combining bond valence calculations and positions of atoms in the layers as well as bridging phosphate units, we arrived at the composition, $[VO_2PO_4 \{P(OH)_2\}_{0\cdot44}]^-$. Difference fourier and bond distance criteria suggested the possible coordinates for N1, C2, C3, and N4. Further refinements with suitable constraints suggested that N1 (4c) is fully occupied while C2, C1 and N2 positions (8d positions) are half-occupied resulting in one ethylene diammonium cation per unit cell. The overall composition, $(H_3NCH_2CH_2NH_3)_{0\cdot5}[V_{0\cdot32}^{4+}V_{0\cdot68}^{5+}O_2PO_4\{P(OH)_2\}_{0\cdot44}]$ agrees well with the chemical analysis and magnetic susceptibility data. Atomic positions and isotropic thermal parameters are given in table 2; selected bond distances and bond angles are listed in table 3.

The structure contains layers made of $V(1)O_5$ square pyramids and $P(1)O_4$ tetrahedra sharing vertices on the *ab* plane. An interesting feature of this structure is that $V(1)O_5$ units on adjacent layers are connected through a disordered tetrahedral $PO_2(OH)_2$ unit;

Table 2. Atomic coordinates $(\times 10^4)$ and equivalent isotropic displacement parameters $(\text{Å}^2 \times 10^3)$ of *en*VPO.

| Atom	x	y	Z	Ueq	Occupancy
V(1)	1740·5(4)	2500·0(0)	2915·1(2)	5·1(1)	1·0
V(2)	1726·9(4)	7500·0(0)	2115·3(2)	5·8(1)	1·0
P(1)	728·3(5)	7·9(5)	7515·9(3)	6·9(1)	1·0
P(2)	2157·8(2)	1642·8(2)	5039·3(6)	8·1(3)	0·4430
O(1)	1723·7(3)	1015·0(6)	6955·6(8)	12·1(4)	1·0
O(2)	1686·3(4)	−915·2(5)	8119·8(8)	11·6(4)	1·0
O(3)	−267·5(4)	995·7(5)	8084·3(8)	12·5(4)	1·0
O(4)	−181·6(4)	−939·3(5)	6916·3(8)	12·1(4)	1·0
O(5)	1777·7(1)	2500·0(0)	1912·7(2)	16·1(6)	1·0
O(6)	1704·3(2)	7500·0(0)	3106·1(2)	16·2(6)	1·0
O(7)	1777·4(0)	7500·0(0)	657·4(3)	22·3(7)	1·0
O(8)	1739·0(0)	2500·0(0)	4304·7(2)	15·2(6)	1·0
O(9)	2806·3(9)	110·4(5)	4681·9(9)	15·9(0)	0·443*
O(10)	694·5(3)	1186·5(3)	5517·7(8)	21·2(1)	0·443*
N(1)	3619·1(1)	2500·0(0)	523·6(6)	25·7(9)	1·0
N(2)	4241·6(3)	254·3(8)	4687·5(5)	12·8(6)	0·5
C(2)	1909·3(0)	−1003·4(4)	5119·3(9)	24·3(5)	0·5
C(1)	3583·5(0)	−1254·5(1)	4944·9(4)	32·6(7)	0·5

*Occupancy of O(9) and O(10) are constrained by the occupancy of P(2) during refinement

Table 3.   Selected bond angles (°) and bond distances (Å) for *en*VPO.

Bond angles

O(8)–V(1)–O(4)	82·21	O(4)–P(1)–O(1)	105·77
O(4)–V(1)–O(4)#1	88·19	N(2)–C(1)–C(2)	107·54
O(4)–V(1)–O(5)	98·63	C(1)–C(2)–N(1)	104·48
O(5)–V(1)–O(2)	98·40	V(1)–O(4)–P(1)	133·07
O(2)–V(1)–O(2)#1	88·08	P(1)–O(3)–V(2)	134·48
O(2)–V(1)–O(8)	80·77	V(2)–O(1)–P(1)	137·32
O(6)–V(2)–O(3)	99·11	P(1)–O(2)–V(1)	131·75
O(3)–V(2)–O(3)#1	89·31	V(1)–O(8)–P(2)	144·05
O(3)–V(2)–O(7)	81·18	P(2)–O(7)–V(2)	129·68
O(7)–V(2)–O(1)	81·59	O(8)–P(2)–O(7)	114·29
O(1)–V(2)–O(1)#1	86·05	O(9)–P(2)–O(10)	105·20
O(1)–V(2)–O(6)	98·11	O(10)–P(2)–O(7)	109·40
O(1)–P(1)–O(2)	109·95	O(9)–P(2)–O(8)	104·80
O(2)–P(1)–O(3)	105·11	P(2)–O(7)–P(2)	57·93
O(3)–P(1)–O(4)	111·79	P(2)–O(8)–P(2)	63·49

Bond distances

V(1)–O(2)	2·0278(1) (×2)	P(1)–O(2)	1·5343(2)
V(1)–O(4)	1·9953(1) (×2)	P(1)–O(3)	1·5511(1)
V(1)–O(5)	1·6022(2)	P(1)–O(4)	1·5177(1)
V(1)–O(8)	2·2208(2)	P(2)–O(7)	1·5752(2)
V(2)–O(1)	1·9409(1) (×2)	P(2)–O(8)	1·4501(2)
V(2)–O(3)	1·9050(1) (×2)	P(2)–O(9)	1·5899(3)
V(2)–O(6)	1·5834(2)	P(2)–O(10)	1·5795(3)
V(2)–O(7)	2·3304(2)	N(1)–C(2)	1·5549(5)
P(1)–O(1)	1·5531(2)	N(2)–C(1)	1·5245(7)
C(2)–C(1)	1·5533(7)		

the unprotonated oxygens of this tetrahedra can also be considered as part of vanadium octahedra with long V–O bond. Each octahedrally coordinated vanadium cation makes one short 'vanadyl' terminal V=O bond ($< 1\cdot62$ Å), and five V–O–P links, each to a different, adjacent phosphorus atom (as a phosphate group). The O7 and O8 atoms that form long V–O bonds with V2 and V1, are strongly bonded to P2 (especially O8: P2–O8 $= 1\cdot45$ Å). The fact that the P2–O7 distance is larger ($1\cdot57$ Å) could be due to the proton around N2 (N2–O7 $= 2\cdot67$ Å). This type of coordination is characteristic of both vanadium (IV) and vanadium (V) compounds. Four of the six phosphate groups (P1–P4) make four P–O–V bonds with nearby V atoms. This VPO configuration results in puckered, $[VO_2PO_4]^{2-}$ layers oriented along the [101] direction (figure 4). The layers are connected by $PO_2(OH)_2$ tetrahedral units to form a three-dimensional network along the *c*-axis. These bonds connect P atoms to the long V–O bond *trans* to the vanadyl V=O link in each case. The two uncoordinated P–O bonds of each of these two phosphate anions are long ($> 1\cdot56$ Å), indicating that they are all protonated (i.e. as H_2PO_4, dihydrogen phosphate groups), as confirmed by FTIR data.
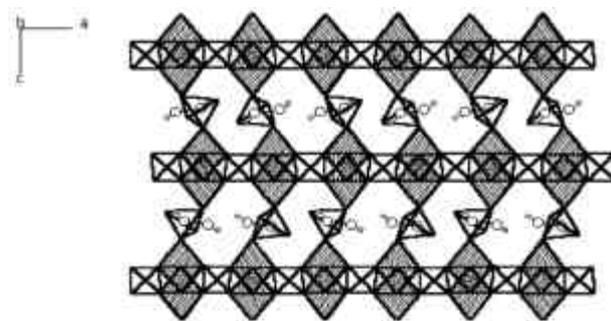
Figure 4. Crystal structure of enVPO viewed along [101].
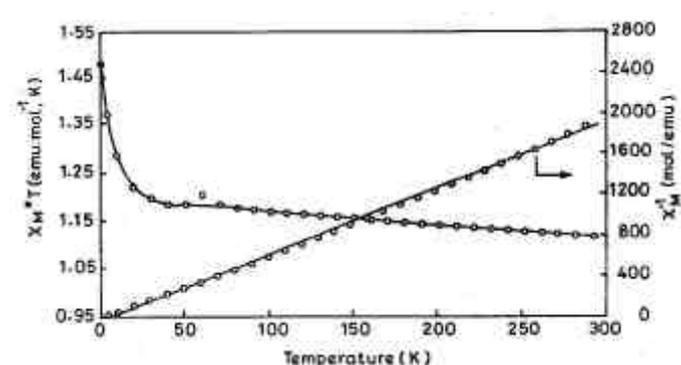
Figure 5. Plot of $c_M T$ and $c_M^{-1} T$ vs T for *en*VPO.

Surprisingly, the composition and structure of *en*VPO appears to be very close to the phase, $(VO)_2(PO_4)_2H_2PO_4.N_2C_2H_{10}$, reported by Harrison *et al*[10]. The cell parameters and the space group of *en*VPO ($a = 9.0289$, $b = 8.8962$ and $c = 15.9813$ Å; *Pnma*) are fairly close to the literature data ($a = 8.891$, $b = 15.971$ and $c = 18.037$ Å; *Pc2$_1$n*) except that the *a*-axis (*c*-axis in the literature) is doubled. If one closely examines our structure, disordering of the phosphate units occurring in between the layers and *en* occurs along the *a*-axis. We re-examined the crystal to determine whether we missed the doubling of the axis. Unfortunately, we did not find any evidence with the CCD diffractometer. Since the composition of our sample indicates a lower V^{4+}/V^{5+} ratio (0.47) in comparison with the literature report (1.0), we believe that the disorder seen in our sample is due to a change in composition.

3.2 *Magnetic property of ethylenediamine intercalated vanadyl phosphate*

Plots of $c_M T$ and inverse molar magnetic susceptibility vs T are shown in figure 5. Magnetic susceptibility data were modelled over the complete temperature range according to the modified Curie–Weiss equation, $1/c_M = (T - q)/[c_0(T - q) + C]$, where c_M is molar magnetic susceptibility, q is Weiss constant, C is Curie constant, T is absolute temperature and c_0 is temperature independent paramagnetism (TIP). The average oxidation state of vanadium calculated on the basis of C_m values is around 4.7 which is

very close to the composition derived from the single crystal structure as well as chemical analysis. The magnetic data reported for the closely related phase,[10] $(VO)_2(PO_4)_2$ $H_2PO_4.N_2C_2H_{10}$, corresponds to a composition with exactly half of the vanadium in the $+4$ state. In this context, magnetic properties of our samples also support the variation in the composition and hence led to a disordered structure as indicated by single crystal analysis. A plot of $c_M T$ versus T is characteristic of ferromagnetic interaction that we observed in NaVPO and AgVPO.[16]

Acknowledgements

References

 1. Centi G, Trifiro F, Ebner J R and Franchetti V M 1998 *Chem. Rev.* **88** 55
 2. Lii K H 1992 *J. Chinese Chem. Soc.* **39** 569
 3. Roca M, Marcos M D, Amoros P, Beltran-Porter A, Edwards A J and Beltran-Porter D 1996 *Inorg. Chem.* **35** 5613
 4. Zhang Y P, Warren C J, Clearfield A and Haushalter R C 1998 *Polyhedron* **17** 2575
 5. Ayyappan P, Ramanan A and Torardi C 1998 *Inorg. Chem.* **37** 3628
 6. Ayyappan P, Ramanan A, Joy P A and Pring A 1999 *Solid State Ionics* **120** 233
 7. Chippindale A M and Cowley A R 1991 *J. Solid State Chem.* **159** 59
 8. Soghomonian V, Chen Q, Haushalter R C and Zubieta J 1993 *Angew. Chem., Int. Ed. Engl.* **32** 610
 9. Riou D and Ferey G 1994 *J. Solid State Chem.* **111** 422
10. Harrison W T A, Hsu K and Jacobson A J 1995 *Chem. Mater.* **7** 2004
11. Zhang Y, Clearfield A and Haushalter R C 1995 *Chem. Mater.* **7** 1221
12. Lu Y, Haushalter R C and Zubieta J 1998 *Inorg. Chim. Acta* **268** 257
13. Zhang D, Shi Z and Feng S H 2001 *Chem. Res. Chinese Univ.* **17** 249
14. Du H B, Liao L B,Yang Z Z and Xiong M 2001 *Acta Chim. Sinica* **59** 274
15. Chippindale A M 2000 *Chem. Mater.* **12** 818
16. Ayyappan P 1999 *Chemistry of intercalated vanadyl phosphates: Synthesis, structure and magnetic properties*, Ph D thesis, Indian Institute of Technology, New Delhi
17. Sheldrick G M 1996 SADABS, a software for empirical absorption correction, University of Göttingen, Göttingen, Germany; SHELXTL Reference Manual, Version 5.03, Siemens Energy and Automation, Inc., Analytical Instrumentation, Madison, WI
18. Brown I D and Altermatt D 1985 *Acta Crystallogr.* **B41** 244